

Widespread Inhibition Proportional to Excitation Controls the Gain of a Leech Behavioral Circuit

Serapio M. Baca,^{1,2} Antonia Marin-Burgin,^{1,2} Daniel A. Wagenaar,^{1,2} and William B. Kristan Jr.^{1,*}

¹Section of Neurobiology, Division of Biological Sciences, University of California, San Diego, La Jolla, CA 92093-0357, USA

²These authors contributed equally to this work.

*Correspondence: wkristan@ucsd.edu

DOI 10.1016/j.neuron.2007.11.028

SUMMARY

Changing gain in a neuronal system has important functional consequences, but the underlying mechanisms have been elusive. Models have suggested a variety of neuronal and systems properties to accomplish gain control. Here, we show that the gain of the neuronal network underlying local bending behavior in leeches depends on widespread inhibition. Using behavioral analysis, intracellular recordings, and voltage-sensitive dye imaging, we compared the effects of blocking just the known lateral inhibition with blocking all GABAergic inhibition. This revealed an additional source of inhibition, which was widespread and increased in proportion to increasing stimulus intensity. In a model of the input/output functions of the three-layered local bending network, we showed that inhibiting all interneurons in proportion to the stimulus strength produces the experimentally observed change in gain. This relatively simple mechanism for controlling behavioral gain could be prevalent in vertebrate as well as invertebrate nervous systems.

INTRODUCTION

Behaviors result from an interplay between excitation and inhibition within the nervous system. Classically, two functions for inhibition were recognized: reciprocal inhibition, with one behavior being inhibited while another is expressed (Eccles, 1969); and lateral inhibition, the shutting down of sensory pathways just outside the area being stimulated, which serves to sharpen the perception of the stimulus (Kuffler, 1953). In recent years, a new form of interaction has been described, namely simultaneous excitation and inhibition (Abbott and Chance, 2005), which has been found in many parts of the vertebrate nervous system (Berg et al., 2007; Haider et al., 2006; Higley and Contreras, 2006; Priebe and Ferster, 2005; Wehr and Zador, 2003), including the spinal cord (Eccles, 1969). Several functions have been suggested for this balanced excitation and inhibition, including the production of response variability (Shadlen and Newsome, 1994; Stevens and Zador, 1998) and the control of spike transmission through the thalamus to the cortex (Wolfart et al., 2005). A recent intriguing possibility is that the balance between

excitation and inhibition onto a neuron affects the *gain* of its response to a given input, because the conductance of the neuron can vary dramatically without changing the membrane potential (Chance et al., 2002). The issue of gain control has attracted recent attention (Salinas and Thier, 2000) for its importance in sensory (Dunn and Rieke, 2006) and motor (Berg et al., 2007; Heckman et al., 2005) processing as well as its likely role in such higher functions as attention (McAdams and Maunsell, 1999), for the coordinate transformations required for visually guided reaching movements (Buneo and Andersen, 2006), and for object recognition in different areas of the visual field (Connor et al., 1997; Salinas and Abbott, 1997).

We wanted to know whether interactions between excitation and inhibition triggered by sensory stimulation in a feedforward network can adjust the gain of a behavioral circuit. To approach this question, we studied how inhibition affects the amplitude of a simple reflexive response—local bending—in the medicinal leech, a response that is elicited by a localized touch and is produced by longitudinal muscle contraction on the side of the touch and relaxation of the corresponding muscles on the opposite side (Garcia-Perez et al., 2004; Kristan, 1982). The response varies with both touch location and touch intensity (Baca et al., 2005). The circuit that generates local bending involves a small number of identified sensory neurons (Lewis and Kristan, 1998a), interneurons (Lockery and Kristan, 1990b), and motor neurons (Kristan, 1982; Lockery and Kristan, 1990a). The only identified central inhibition in this circuit is provided by the connections from the inhibitory motor neurons onto the excitatory motor neurons (Figure 4A) (Granzow and Kristan, 1986; Lockery and Kristan, 1990a). These inhibitors release GABA in a graded, spike-independent manner centrally onto the contralateral excitators (Cline, 1986; Cline et al., 1985; Granzow et al., 1985) and peripherally onto longitudinal muscle fibers (Stuart, 1969, 1970). The connections were thought to produce an effective lateral inhibition that focused the excitation at the site of the touch and relaxed the opposite side to produce the bend (Kristan et al., 1995).

This circuit is an appropriate one to study gain control for several reasons. First, at a behavioral level, mechanical stimuli of increasing magnitude produce increasingly large responses (Baca et al., 2005; Thomson and Kristan, 2006). Second, the underlying circuit is a three-layered, feedforward network composed of a small number of identified neurons (Kristan, 1982; Lewis and Kristan, 1998a; Lockery and Kristan, 1990a; Lockery and Kristan, 1990b). Third, perturbing the activity of any of the individual neurons affects the expression of the behavior, thereby showing the behavioral significance of each neuron (Briggman et al., 2005;

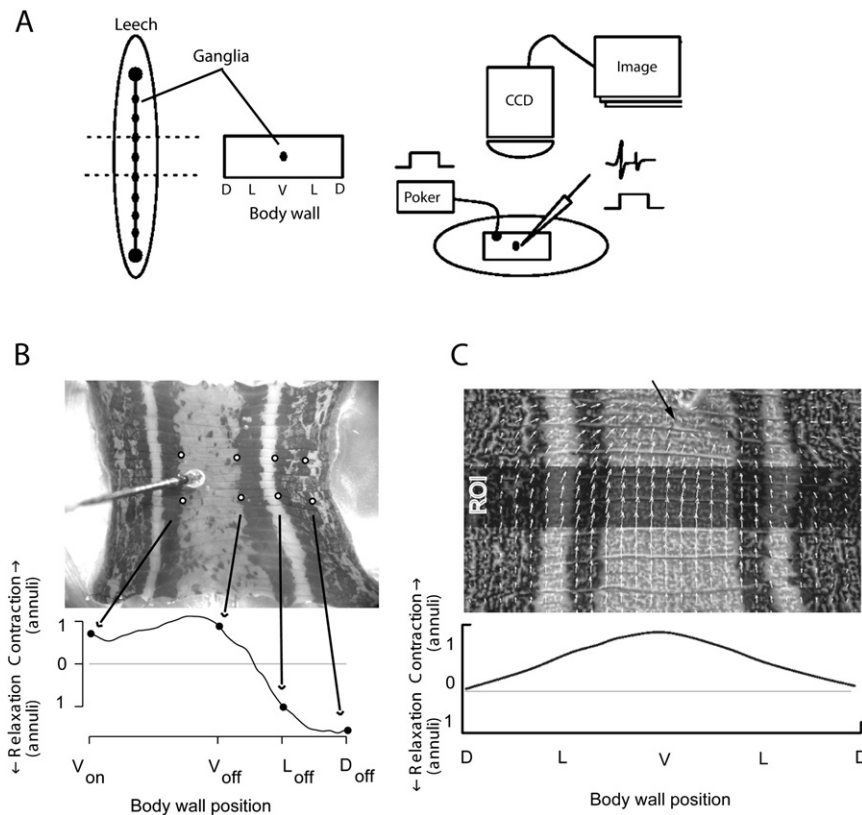


Figure 1. Generating and Recording Local Bending Responses

(A) Schematic diagram of a leech, indicating the location of its central nervous system: head and tail brains (depicted as large dots at anterior and posterior ends) with 21 segmental ganglia (smaller dots) in the ventral nerve cord. To record local bending, we cut open the body wall of segments 8–12 along the dorsal midline and pinned it down, outside up, on a Sylgard substrate. This creates a flat piece of body wall with the cut dorsal midline at the lateral edges. We removed ganglia 8, 9, 11, and 12, leaving only ganglion 10 connected to the body wall. We recorded movements from above using a CCD camera mounted on a dissecting microscope, digitized the images, and stored them on a computer. We delivered mechanical stimuli using an electronically controlled poker with a surface area of about 1 mm^2 . The duration of each stimulus was either 3 s (Figure 2) or 0.5 s (all other experiments); stimuli were spaced 3 min apart to prevent response adaptation.

(B) Loosely pinned preparation used to generate local bending. We manually chose points along the edges of the five annuli corresponding to the innervated segment in the first frame in each of the movies (the most anterior and posterior points are indicated by arrows) and used an optical flow-detection algorithm (Ye and Haralick, 2000) to track the motion of these markers. The distance between the anterior and posterior markers 0.5 s after withdrawal of the stimulator was compared to the distance just before stimulation. The trace

below the body wall image is a smoothed version of the change of distance between the anterior and posterior markers at each of four locations at 0.5 s after withdrawing the stimulus. V_{on} is the on-target ventral location of the stimulus; V_{off} , L_{off} , and D_{off} are off-target locations in ventral, lateral, and dorsal locations whose movements we plotted. The distance moved was initially measured in units of pixels, which were then normalized to annuli by measuring the number of pixels per annulus.

(C) Tightly pinned preparation used to record local bending and neural activity. We measured movements in a selected region of interest (ROI) away from the stimulus site (arrow), to avoid optical and mechanical artifacts caused by movements of the poker. The ROI is indicated as a dark swath across the middle of the image. We represented movements of 80 to 240 locations in a grid within the ROI as vectors. We averaged the lengths of the vector components parallel to the long axis of the body wall at 20 to 80 locations and smoothed this result to obtain a bend profile (graph below the body wall image). Again, the magnitudes of the movements were normalized to the number of annuli.

Heinzel et al., 1993; Kristan et al., 1982; Stent et al., 1978; Zoccolan and Torre, 2002). Fourth, local bending depends on a population of distributed interconnections that include inhibitory connections (Kristan et al., 1995).

We performed behavioral experiments while recording from neurons with intracellular microelectrodes and voltage-sensitive dyes (Cacciatore et al., 1999). We monitored the activity of many neurons at once while knocking out inhibition both pharmacologically and electrophysiologically. We found that GABAergic inhibition among the motor neurons produced both lateral inhibition, as previously shown (Granzow and Kristan, 1986; Lockery and Kristan, 1990a), as well as a generalized inhibition of most neurons in the CNS. This generalized inhibition was responsible for setting the gain of the response, which provided the broad dynamic range of the response to different levels of sensory stimulation. These results show that very localized sensory stimulation of the leech's skin produces a balanced excitation and inhibition that sets the gain of the response. The experiments and modeling suggest that this inhibition is strong and uniform across all interneurons, and possibly all motor neurons, in the ganglion.

RESULTS

Role of GABAergic Inhibition on Local Bending

To establish the input-output function for local bending at a given stimulus site, we used a loosely pinned, flattened body wall preparation that was innervated by a single ganglion (Figure 1B). To induce local bends, we applied tactile pulses of constant force to the skin for 3 s and used an optic flow algorithm to measure the resulting body movements (Ye and Haralick, 2000; Zoccolan and Torre, 2002) along four lines of longitudinal markers at 0.5 s after releasing the stimulus. We applied stimuli to the middle of either the right or left ventral surface (i.e., half-way between the ventral midline and the lateral edge) because previous studies (Baca et al., 2005; Thomson and Kristan, 2006) have shown that these sites produced easily distinguishable bend profiles in body wall preparations. For each of ten leeches, we applied two or three stimuli at each of ten force levels between 0.75 and 400 mN. We then washed in a solution of 0.1 mM bicuculline methiodide (BMI). Access of BMI to the ganglion was ensured by applying it from below the pinned-out body wall through an inlet

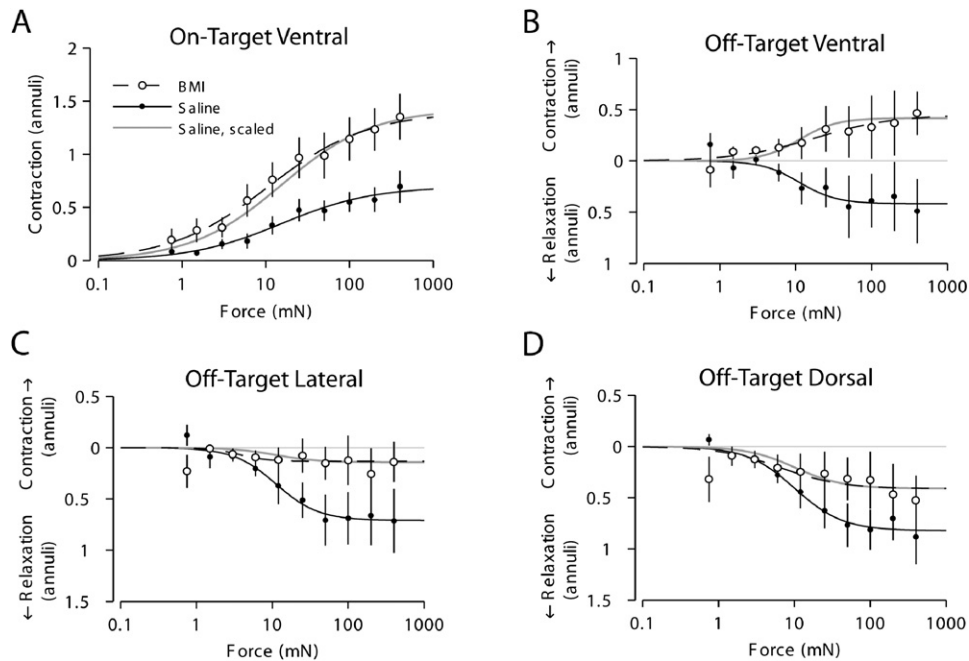


Figure 2. The Effects of GABAergic Inhibition on the Magnitude of Local Bend Responses

(A) Responses of the on-target contractions in the ventral body wall to mechanical stimulation at a single midventral site in normal saline (filled circles) and in saline with 0.1 mM BMI (open circles). The black solid line is a sigmoid fit of the responses in saline, the dashed line is the sigmoid fit to the responses in BMI, and the gray line is the black line multiplied by 2.1. The remaining three graphs are similar plots from responses recorded at three different contralateral off-target sites: ventral (B), lateral (C), and dorsal (D). The gray lines are the black lines multiplied by -1.0 (B), 0.2 (C), and 0.5 (D). In all graphs, the magnitudes of the movements were normalized to the number of annuli. All experiments were repeated in ten preparations.

The values shown in all panels are mean \pm SEM.

built into the Sylgard substrate. In pilot experiments, the effect of BMI was robust within 10 min, so we waited 10 min after application of BMI before repeating the stimulation protocol.

In control conditions, each touch produced a longitudinal contraction of the on-target ventral body wall at all intensities used, accompanied by relaxation of the off-target ventral, lateral, and dorsal body wall locations (Figures 2A–2D, filled circles). The responses in all four locations were well fit by sigmoid curves (solid lines). The on-target responses were contractions that increased in amplitude with increasing stimulus intensity, plateauing at about 0.8 annuli of shortening. The off-target responses were, on average, relaxations whose amplitudes saturated at -0.4 (Figure 2B), -0.7 (Figure 2C), and -0.8 (Figure 2D) annuli in ventral, lateral, and dorsal locations.

Bath application of BMI greatly increased the magnitude of the on-target contractions, even at low force levels (Figure 2A, open circles), and decreased the relaxations at the three off-target sites (Figures 2B–2D, open circles). In fact, the relaxations observed at the off-target ventral site in control conditions became contractions in the presence of BMI (Figure 2B). To measure the size of the change induced by BMI, we multiplied the sigmoid curve obtained for the control responses by a value that made its plateau value equal to the sigmoid obtained in BMI. The multiplier values required were 2.1 (Figure 2A), -1.0 (Figure 2B), 0.2 (Figure 2C), and 0.5 (Figure 2D). These scaled values are shown as solid gray lines in Figures 2A–2D. The fact that the scaled curves were within one standard error of the observed data

at every stimulus intensity at all four locations indicates that BMI increases the amplitude of the response uniformly over the whole range of stimulus intensities. In other words, the inhibition blocked by BMI changes the gain of the whole system.

To determine whether the BMI was having its major effects on the central nervous system or at the inhibitory connections onto the muscles (Stuart, 1970), we used a split body wall preparation (Figure 3A) with a Vaseline well built around the ganglion. We applied BMI either to the ganglion inside the Vaseline chamber or to the body wall outside the chamber. The results to BMI application at the two locations were very distinct (Figure 3): applying BMI to the body wall alone did not affect either the on-target or the off-target responses (even with 1.0 mM BMI), but applying 0.1 mM BMI to the ganglion produced a larger contraction at both sites, both in individual (Figure 3A) and averaged responses (Figure 3B). In fact, the on-target and off-target responses were not significantly different in the presence of BMI. This experiment leads to two conclusions: (1) the increased magnitudes of the local bending responses produced by BMI on the body wall (Figure 2) were due entirely to blocking inhibition within the ganglion; and (2) the contributions of peripheral inhibition to local bending responses were unaffected by bath application of BMI.

Why BMI did not affect inhibition within the body wall might have three causes: (1) the BMI might not gain access to the neuromuscular junctions, (2) the GABA receptors on the muscles might be insensitive to BMI, or (3) the inhibitory terminals on

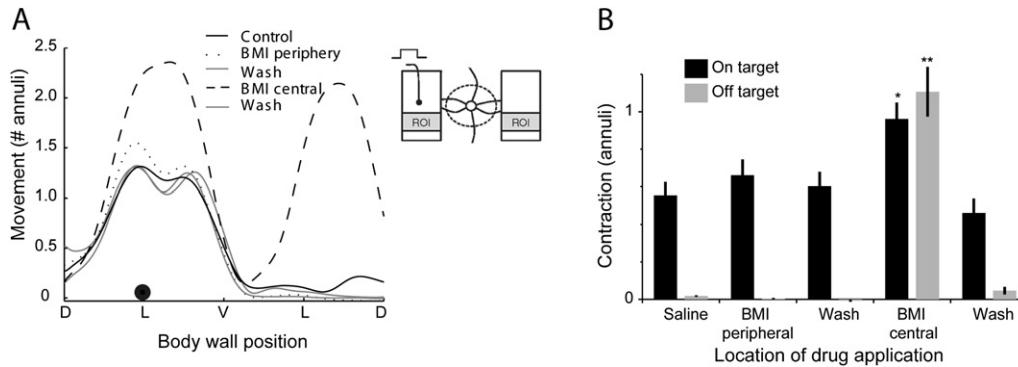


Figure 3. Bath-Applied BMI Blocks GABAergic Inhibition Centrally, Not Peripherally

(A) Using a split body wall preparation (icon) with a Vaseline wall around the ganglion, we delivered mechanical stimuli at a single location (left lateral edge) and a single intensity (200 mN). We measured the bend profiles before adding BMI (Control), after adding BMI to the saline bathing the body wall (BMI Periphery), after adding BMI to the saline bathing the ganglion (BMI Central), and after replacing the BMI with saline (Wash) after each BMI addition. This example shows a strong contraction on the side stimulated and a weak contraction on the opposite side. When BMI was applied, the on-target response nearly doubled in size and the off-target response became nearly as large as the on-target response. The fact that there is no contraction in the middle of the graph is an artifact of the preparation: the body wall was split up the ventral midline to provide access to the ganglion; the optic flow algorithm detected no movement in this region. We measured on-target and off-target amplitudes at the peaks, which were in sites minimally affected by the midventral incision.

(B) Quantification of the BMI effects on the ganglion and on the body wall ($n = 10$). The values shown are mean \pm SEM. Adding BMI to the saline bathing only the body wall (BMI Peripheral) did not change either the on-target or the off-target response, whereas adding BMI to the saline bathing the ganglion (BMI Central) produced a significant increase in both the on-target and off-target responses compared either to pre-BMI application conditions (Saline) or after washing out the BMI (Wash) (ANOVA, $p < 0.001$; post hoc t tests for individual comparisons, $p < 0.01$).

muscles might be non-GABAergic. Whatever the cause, however, the nonblocked peripheral inhibition is the most likely explanation for the residual relaxation seen at lateral and dorsal body wall sites (Figures 2C and 2D).

Hyperpolarizing the Inhibitors Broadens the Local Bending Response

From previous studies (Kristan, 1982; Lewis and Kristan, 1998a; Lockery and Kristan, 1990b), the known local bend circuitry in each segment is a three-layered, feedforward circuit consisting of just four sensory neurons (pressure-sensitive P cells), about two dozen local bend interneurons (LBIs), and about the same number of longitudinal motor neurons (Figure 4A). All the connections indicated are excitatory chemical connections except for the connections from the inhibitory motor neurons (DI and VI) onto the corresponding excitatory motor neurons (DE and VE); these are GABAergic inhibitory connections (Cline, 1986). To evaluate whether BMI exerted its effects by blocking these known inhibitory connections, we removed this inhibition from the circuit reversibly by strongly hyperpolarizing one of them. This is an effective procedure because all the inhibitory motor neurons are strongly electrically coupled to one another (Figure 4B) (Granzow et al., 1985; Lockery and Kristan, 1990b; Ort et al., 1974). We stimulated the skin while hyperpolarizing the inhibitor DI-1 throughout the local bend response, using a *hole-in-the-wall* preparation (Figure 4C). In this example, the off-target response increased while the inhibitors were hyperpolarized, but the amplitude of the on-target response did not change. Statistical comparisons of responses from ten preparations (Figure 4D) showed that the off-target increase was significant and that the on-target responses were not different. This result shows that the central connections of the inhibitors onto the excitators functioned only to restrict the contraction to the side

touched; in other words, the inhibitory connections among motor neurons produce lateral inhibition but do not contribute to the generalized inhibition.

Role of GABAergic Inhibition on Neuronal Responses Effects on Motor Neurons

To determine how generalized inhibition affects the central nervous system, we recorded intracellularly from motor neurons while stimulating one of the four mechanosensory neurons that triggers local bending. Previous studies (Kristan, 1982; Lockery and Kristan, 1990b) have shown that stimulating a single P cell excites the excitatory longitudinal motor neurons with their motor fields in the same area as the touch (i.e., the on-target excitators), inhibits the excitatory longitudinal motor neurons on the opposite side (the off-target excitators), and elicits a mixed response in excitators with intermediate movement fields (the intermediate excitators). We replicated these findings using both electrophysiological and imaging techniques (Figure 5). We stimulated a single P cell at 10 Hz for 500 ms (comparable to delivering moderate mechanical stimuli to the body wall [Lewis and Kristan, 1998b]) and repeated this stimulus train once per second for ten cycles, to produce a signal detectable by the voltage-sensitive dyes (VSDs). When, for example, we stimulated a P_V neuron—one of the two P cells that innervates ventral leech skin—the on-target VE-4 motor neuron was excited (Figure 5D), the off-target DE-3 motor neuron was inhibited (Figure 5A), and the two intermediate excitatory motor neurons (Figures 5B and 5C) received smaller excitation than the on-target motor neuron. These same features were seen in all seven cases tested, in both the electrophysiological and the VSD recordings. (Note that the cyclic membrane potential changes are captured in the VSD recordings, but the faster membrane potential shifts

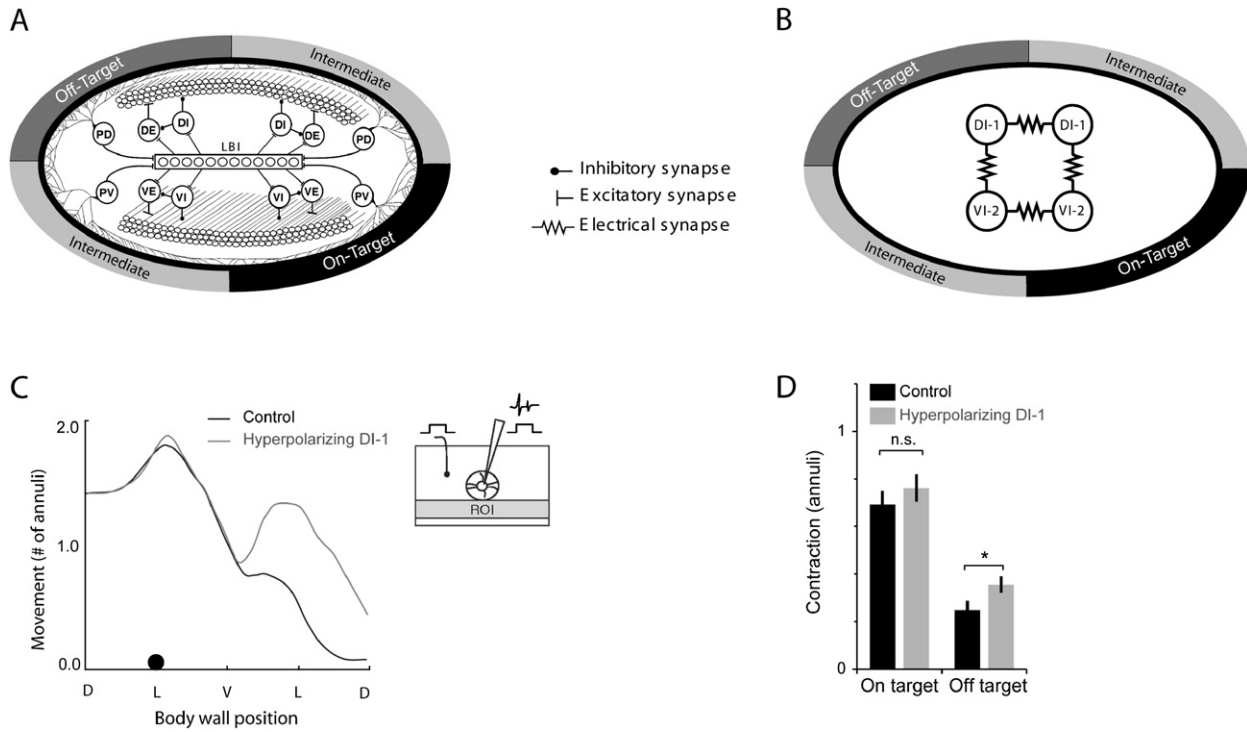


Figure 4. Removing Inhibition Among Motor Neurons by Hyperpolarizing the Inhibitors Increased the Off-Target Response but Did Not Affect the On-Target Peak Amplitude

(A) Simplified version of the local bend circuitry (Kristan, 1982; Lewis and Kristan, 1998a; Lockery and Kristan, 1990b). Just four pressure-sensitive mechanoreceptive neurons (a P_D and a P_V on each side) innervate overlapping regions of the skin, with the centers of their receptive fields in the middle of the two dorsal (D) or ventral (V) regions. All four P cells excite a collection of local bend interneurons (LBIs), which in turn excite the motor neurons to the longitudinal muscles. There are two functional types of motor neurons, excitatory (E) and inhibitory (I), that innervate either the dorsal (D) or ventral (V) longitudinal muscles. All identified connections are feedforward and excitatory, except for those made by the inhibitory motor neurons, which make GABAergic inhibitory synapses onto both the appropriate longitudinal muscles and the corresponding excitatory motor neurons. Hence, there are four types of motor neurons (DE, DI, VE, and VI) on each side. (The somata of all neurons are in a ganglion on the ventral surface of the segment; they are shown in the middle of the body in this diagram for clarity.) Motor neurons causing muscle contractions in the quadrant whose P cell was stimulated are “on-target,” and the ones on the side opposite to the stimulation are “off-target.”

(B) Schematic version of the electrical connections among the inhibitory motor neurons. Because they make nonrectifying electrical connections to one another, hyperpolarizing one inhibitor hyperpolarizes all of them. (Not shown: DE cells make nonrectifying electrical connections to other DEs, and VEs make nonrectifying electrical connections to other VEs; these connections are not represented in either diagram.)

(C) We used the hole-in-the-wall preparation (icon) to impale inhibitory motor neurons while eliciting local bending. We stimulated a single site (black dot on the x axis) and a single intensity (200 mN) while strongly hyperpolarizing a single inhibitor, thereby inactivating all the inhibitory motor neurons via widespread electrical connections. Mean bend profiles are shown for one preparation before (solid black line) and while (grey solid line) passing -2 to -7 nA of hyperpolarizing current into an inhibitory motor neuron.

(D) The peak amplitudes of the on-target responses were not affected by hyperpolarizing the inhibitory motor neurons ($p > 0.40$), whereas the off-target responses were significantly increased by these hyperpolarizations ($p < 0.04$).

were lost because of the slow time constant of the dyes [Cacciatore et al., 1999].

We then stimulated the same neuron after changing the bathing solution to saline containing 0.1 mM BMI to block GABAergic inhibition. As in the behavioral experiments (Figure 2), blocking GABAergic inhibition increased the excitation made by P_V onto all excitatory motor neurons (right-hand panels in Figures 5A–5D, with a light gray background): neurons that had received excitation in control conditions (Figures 5B and 5D) received significantly larger excitation in the BMI saline, and those that had been inhibited were now excited. These effects of BMI were observed in all seven preparations tested. These results show that increases in the behavioral responses induced by BMI (Figure 2) are apparent in the responses of the excitatory motor neurons.

We were concerned that BMI application might produce an excitatory effect on neurons in the circuit, as has been seen in mammalian neurons (Seutin and Johnson, 1999). To control for such a direct effect of BMI on leech neurons, we applied 100 μ M BMI to isolated ganglia while monitoring the membrane potential and the input resistance of sensory neurons, interneurons, and motor neurons—both excitatory and inhibitory—in the local bend circuit. BMI application did not affect the membrane potential of mechanosensory P cells (they depolarized by 0.5 ± 1.7 mV, $n = 5$). BMI application slightly hyperpolarized interneurons and motoneurons: interneuron 212 hyperpolarized 4.5 ± 1.2 mV ($n = 3$); excitatory motor neurons DE-3 and VE-4 hyperpolarized 5.7 ± 1.6 mV ($n = 4$) and 4.5 ± 2.0 mV ($n = 4$), respectively; and the inhibitory motor neurons DI-1 and VI-2

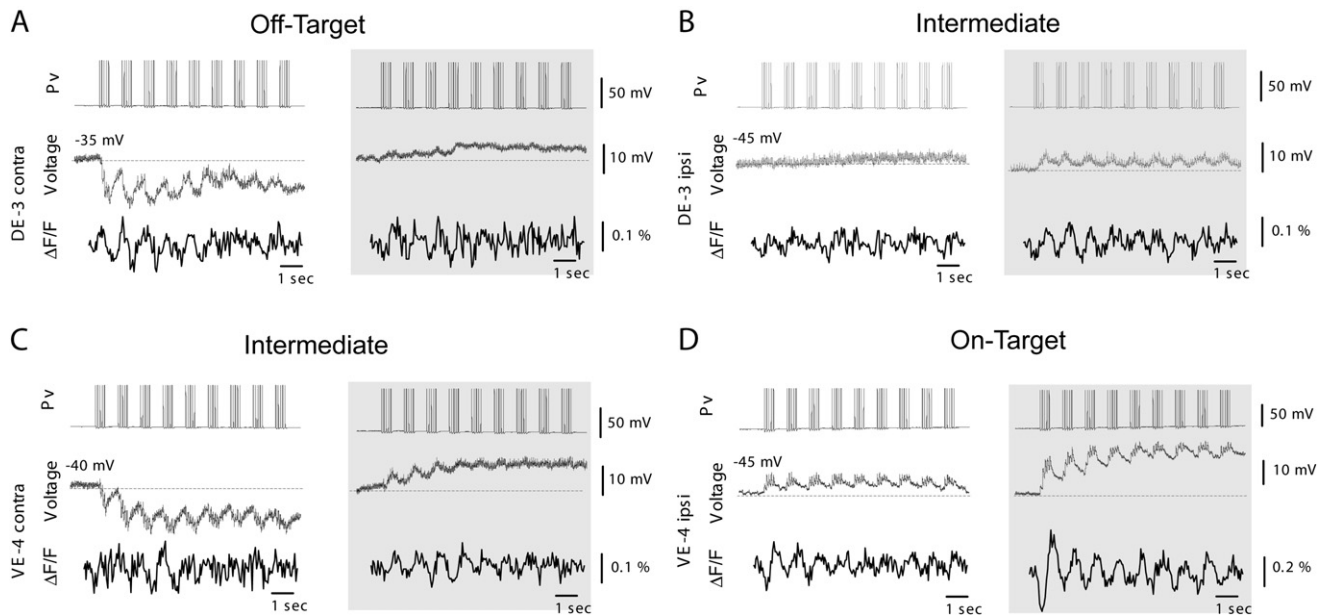


Figure 5. Effects of Bicuculline Methiodide on the Responses of Longitudinal Excitatory Motor Neurons (DEs and VEs) to P Cell Stimulation

In panels (A)–(D), the top traces show the times when spikes were generated in the right P_V neuron, the middle traces are intracellular recordings from either a DE or a VE, and the bottom traces are voltage-sensitive dye recordings obtained from the motor neuron simultaneous with the intracellular recording just above it. The VSD units are percent change in amplitude of the fluorescent signal ($\Delta F/F \times 100\%$). In every panel, the traces on the left were obtained while the ganglion was bathed in standard saline, and the traces on the right (against a gray background) were obtained from the same neuron after replacing the saline with one containing 0.1 mM BMI.

- (A) Intracellular and VSD recordings from the contralateral cell DE-3, an off-target excitor of left dorsal longitudinal muscles.
 (B) Intracellular and VSD recordings from the ipsilateral cell DE-3, an intermediate excitor of right dorsal longitudinal muscles.
 (C) Intracellular and VSD recordings from the contralateral cell VE-4, an intermediate excitor of left ventral longitudinal muscles.
 (D) Intracellular and VSD recordings from the ipsilateral cell VE-4, an on-target excitor of the right ventral longitudinal muscles.

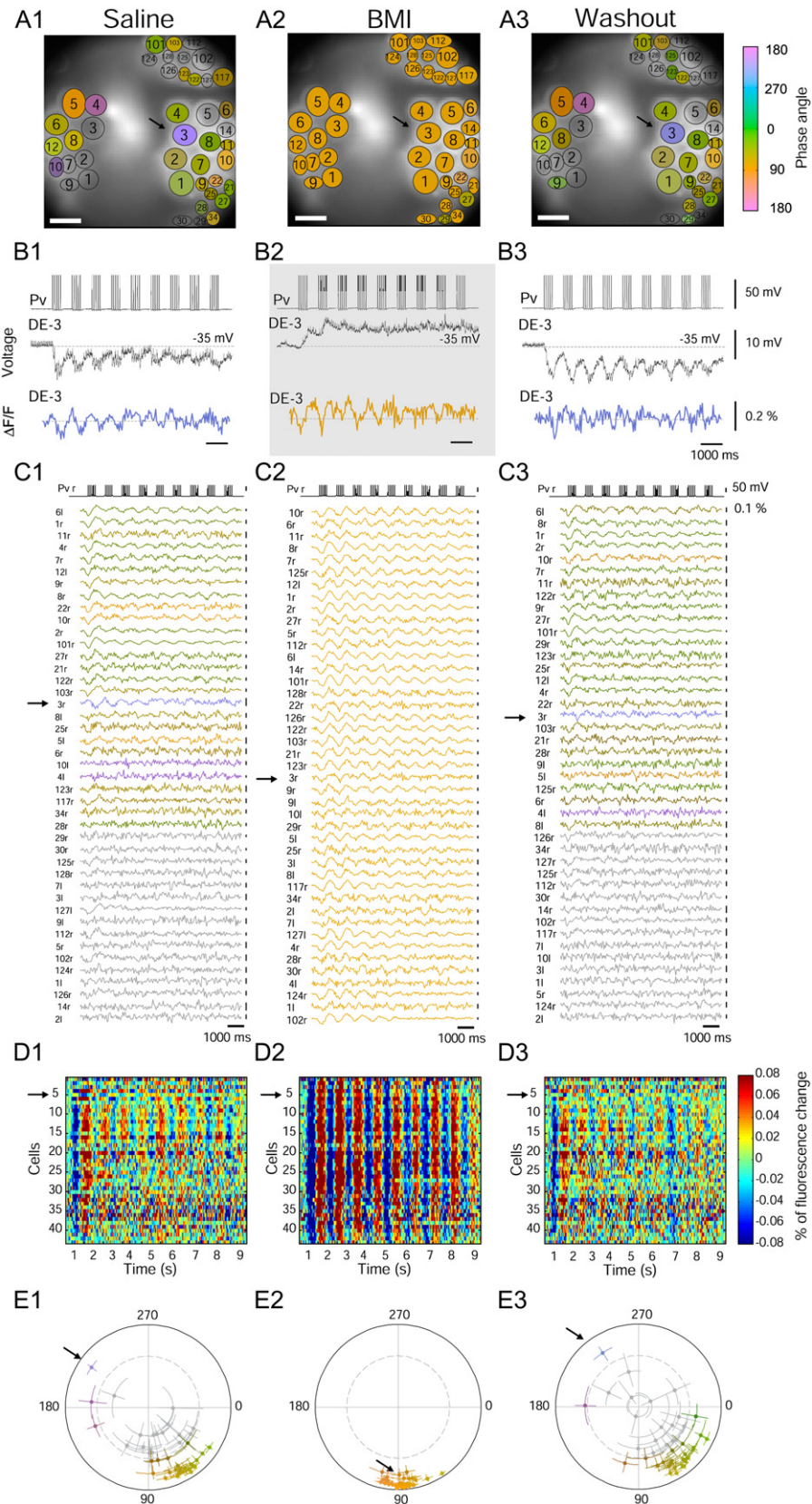
hyperpolarized 5.4 ± 1.5 mV ($n = 4$) and 5.3 ± 0.9 mV ($n = 3$), respectively. BMI did not produce any significant change ($p > 0.05$, t test) in the input resistance of any of these recorded neurons. Hence, the only direct effect of BMI onto the neurons in this circuit was inhibitory, an effect opposite to the generalized excitation seen in local bending after applying BMI. These results showed that the increased excitation in the network seen after BMI application, therefore, were not caused by direct excitatory effects of BMI on the neurons in the circuit.

Effects on Other Neurons

Because we were imaging all the neurons visible on the dorsal surface of the ganglion with the VSDs while recording from the excitatory motor neurons electrophysiologically, we could also determine the activity of another 40 to 50 neurons (Figure 6). In standard saline (left panels of Figure 6), the intracellular recordings (Figure 6B) and the trajectories of the optical signals from the imaged neurons (Figures 6C and 6D) show that many of them respond to each P cell spike burst, seen as oscillations at the same frequency as the stimulus bursts. Those that were phase locked to the stimulus were active in different phases of the stimulus cycle. This phase locking was quantified using polar plots (Figure 6E) that show both the phases (distance around the circumference) and the coherence magnitudes (distance from the center) for all visible neurons (Cacciatore et al., 1999). Neurons with significant coherence values (outside the dashed lines in Figure 6E) have been colored in the ganglionic images

(Figure 6A) and in the individual trajectories (Figure 6C). Brighter colors represent higher coherence values, and different hues represent the phases of the responses relative to the stimulus. The neurons that were phase locked to the stimulated P_V cell in normal saline clustered in two distinct phases (Figure 6E), corresponding to excitation (clustered between 45° and 90°) and inhibition (scattered points around 180°).

We then repeated the same P_V stimulation regime after replacing the bathing solution with saline containing 0.1 mM BMI (Figure 6, middle panels). With all GABAergic inhibition blocked, every neuron had large-amplitude, phase-locked oscillations in the VSD trajectories (Figures 6C2 and 6D2) that clustered around 90° (Figure 6E2), indicating that the P_V spike bursts now excited all the neurons. (The peak of the excitatory responses were, on average, more delayed in BMI than in control because the inhibition caused by each stimulus train occurred later than the excitation; therefore, blocking the inhibition selectively enhanced the later part of the excitatory response, which produced the observed delay in the peak excitation.) One example of a switch in the nature of the response is provided by the off-target cell DE-3 (arrow in Figure 6E2), which switched its phase from 220° to 90° . This switch is also apparent in the intracellular recordings (Figures 6B1 and 6B2). Comparing the left and middle panels of Figure 6 shows that approximately half the neurons were significantly coherent with the spike bursts in normal saline, with most of these being excited and the rest inhibited. After removing the



GABAergic inhibition with BMI, the P_V stimuli strongly excited every neuron. We did not see consistent or large changes in the membrane potential or in the spontaneous activity of the neurons recorded intracellularly when BMI was added, indicating that the major changes in response patterns in BMI saline required sensory stimulation. The effects of BMI reversed within 10 min after washing the ganglion with normal saline (right panels of Figure 6).

To be sure that the BMI did indeed block inhibition, we stimulated inhibitors through intracellular electrodes and found that BMI was very effective in blocking their central inhibitory effects on excitors (data not shown). Interestingly, many neurons that were clearly inhibited by the inhibitors in saline were found to be excited by them in the presence of BMI, possibly by their electrical connections. Such dual electrical and chemical connections between neurons have been observed in the leech CNS (Nicholls and Purves, 1970; Ort et al., 1974), as well as in other nervous systems (Hatton, 1998; Mamiya et al., 2003; Moss et al., 2005).

It should be noted that included in the many neurons that were excited by P_V stimulation with BMI present were the inhibitory motor neurons. In fact, the inhibitors would be more strongly activated by P_V stimulation in the presence of BMI—because the central inhibition onto them would be blocked (Figure 6) but their peripheral inhibition would not be affected (Figure 3)—so that they would generate more relaxation of the muscles. Hence, the difference between the BMI and control curves in Figure 2 is likely to be an underestimate of the effect of central inhibition.

Contribution of Inhibitory Motor Neurons in the CNS Expression of Local Bending

We determined whether the known inhibitory connections from inhibitors onto excitors contributed to the generalized inhibition by strongly hyperpolarizing one of them, in the same way that we had previously tested for the effects of this inhibition on local bending behavior (Figure 4). For these experiments, we imaged the dorsal surface of each ganglion with VSDs while stimulating a P_V cell before, during, and after hyperpolarization of the inhibitors (Figure 7). In control recordings before and after hyperpolarizing cell DI-1, the responses of the neurons to P_V stimulation (Figures 7B1 and 7B3) were comparable to the responses in Fig-

ures 6D1 and 6D3: many neurons were excited (i.e., their activity phases were between 0° and 90°), and a few were inhibited (phases were around 270°). During cell DI-1 hyperpolarization, however, P_V stimulation no longer inhibited any imaged neurons, and the excited neurons were more tightly clustered around 45° (Figure 7C2). As indicated by the arrows in Figures 6C1–6C3, hyperpolarizing the inhibitors inverted the response of the off-target excitors: normally inhibited by P_V stimulation, they were excited during hyperpolarization of the inhibitors in 6 of 6 experiments. However, hyperpolarizing the inhibitors did not produce an effect as widespread as that produced by BMI (compare Figure 7B2 to Figure 6D2), strengthening the conclusion that the central effects of the inhibitory motor neurons do not contribute to the generalized inhibition documented in Figures 2 and 6.

The differences between application of BMI and hyperpolarizing the inhibitors are quantified in Figure 7D. Application of BMI significantly increased the number of cells excited by P_V stimulation, measured as the number of neurons significantly coherent with the stimulus (one-way ANOVA, $F_{3, 33} = 12.11$, a posteriori Tukey test $p < 0.001$; $n = 7$). Hyperpolarizing the inhibitor cell DI-1 did cause an increase in the number of neurons excited by P_V stimulation compared to control ($p < 0.05$; $n = 6, 7$, respectively), but this number was less than the number excited by P_V stimulation during BMI application ($p < 0.05$). The values for both conditions after ending the treatment (BMI application or hyperpolarization) were not different from control.

A Model with Generalized Feedforward Inhibition Reproduced the Major Behavioral Results

To test whether the observed generalized inhibition could change the gain of the output by acting on the interneurons, we modeled the input-output functions of the local bending circuit with and without the generalized inhibition, to mimic the effects of blocking inhibition with BMI (Figure 8A). In particular, we wanted to capture the two major features of the behavioral experiments (Figure 2): (1) blocking the GABAergic inhibition caused a 2-fold increase in the whole stimulus-response curve, whereas (2) the minimal touch intensity needed to cause a response did not change detectably. We used a simplified network model (Figure 8A1), consisting of a mechanosensory P cell (P), which excites a local bend interneuron (LBI), which in turn excites

Figure 6. Effects of Bicuculline Methiodide on the Responses of All Neurons on the Dorsal Surface of a Midbody Ganglion

(A) Images of the dorsal surface of a midbody ganglion used to record neuronal activity with voltage-sensitive dyes. Hand-drawn ellipses indicate the boundaries of neuronal somata. The numbers were assigned according to the positions of the somata on a standard ganglionic map (Muller et al., 1981). The colors indicate the phase of the VSD trajectories of each neuron relative to the stimulus burst cycles, as determined by the phase plots in (E1)–(E3) below. The arrows here and in panels (C)–(E) identify the cell DE-3 that was recorded intracellularly. Scale bars, 50 μm .

(B) The top traces are intracellular recordings from a P_V cell (outside the field of view in panel [A]) showing when trains of five action potentials were evoked by depolarizing current pulses (5 nA, 7 ms, 10 Hz) generated for 500 ms at 1 Hz. Simultaneous intracellular recordings (middle traces) and optical trajectories (bottom traces) show the responses of the indicated cell DE-3. The colors of the optical traces correspond to the phases of the response (from panel [E]): blue indicates inhibition, and gold indicates excitation. The B2 recordings are responses of DE-3 to the same P_V stimulation with 0.1 mM BMI in the bathing solution.

(C) Recordings of the driven spike burst in the P_V cell (top trace) along with fluorescence signals from the 43 cells visible in the ganglion (A1–A3). Colors of the fluorescence traces correspond to phasing of the responses (from [E1]–[E3]); gray traces indicate noncoherent neurons. Calibration bars are displayed below and to the right of the recordings. Signals are lined up in decreasing order of their coherence values, with the maximum value (with the largest oscillation amplitude) at the top.

(D) Optical recordings from the same 43 neurons, with response valence indicated by color: red indicates depolarization to each burst, and blue indicates hyperpolarization to each burst (color bar to the right of [D3]).

(E) Polar plots indicate the coherence phase (circumferential distance from 0°) and magnitude (linear distance from the center of the plot) for all neurons observed in the image. Each point indicates the average phase and maximal amplitude of a single neuron; the lines from each point indicate the standard errors in both amplitude and phase about the mean. Neurons with amplitude values greater than the dashed line are coherent with the stimulus at the 95% confidence limit.

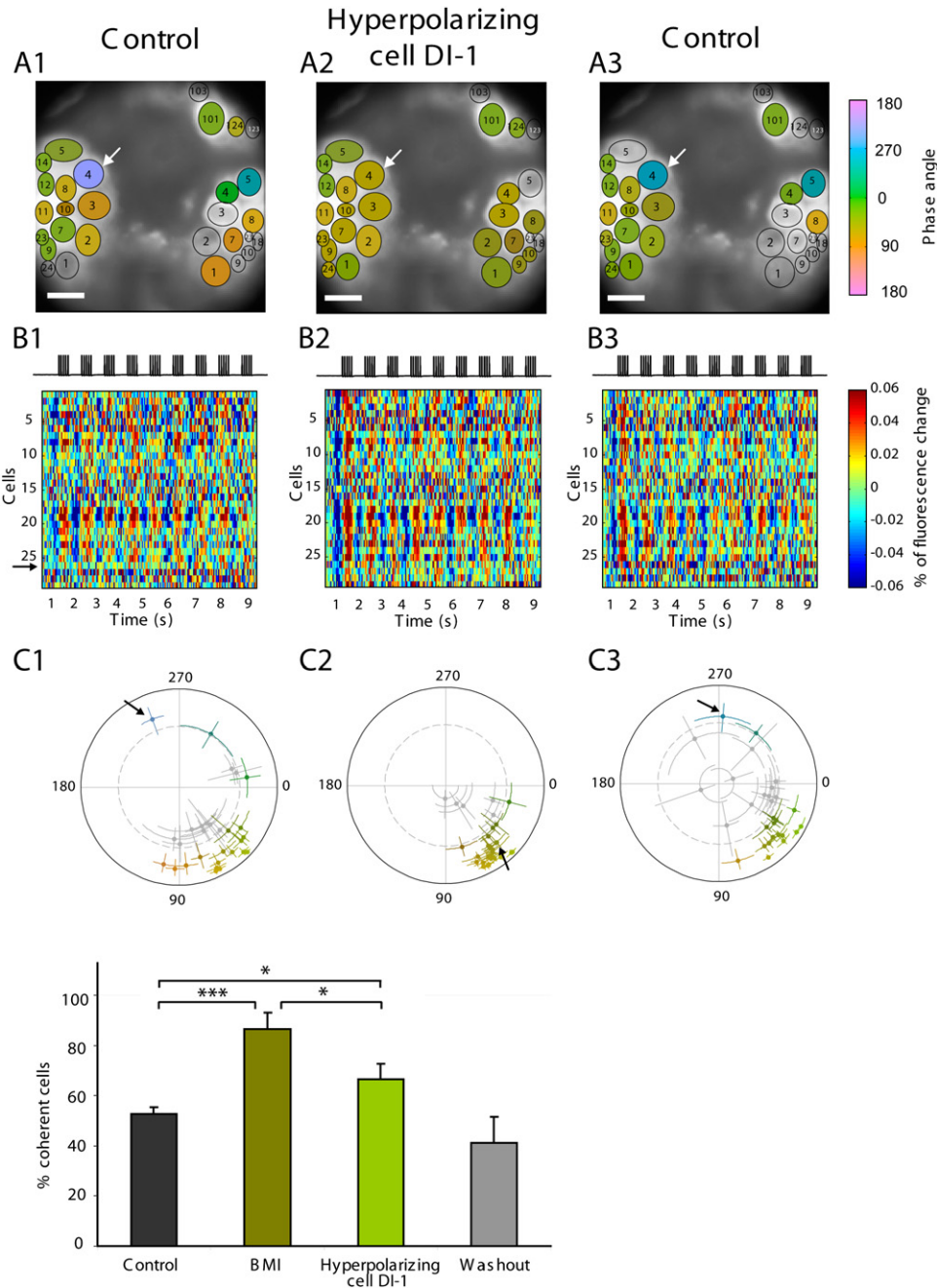


Figure 7. Effects of Removing Inhibition, by Hyperpolarizing the Inhibitor Responses, on All Neurons on the Dorsal Surface of a Midbody Ganglion

(A) Images of the dorsal surface of a midbody ganglion used to record neuronal activity with voltage-sensitive dyes. As in Figure 2, we impaled a mechanosensory P_v neuron (outside the field) and elicited a train of spikes at 10 Hz for 500 ms, repeated every second for 10 s. The color of each neuron indicates the phase of its response relative to the stimulated neuron (C1–C3). Experiments were performed without passing current into the DI-1 neuron (Control), during the time that cell DI-1 was hyperpolarized with -5 nA, then again not passing current into DI-1. Scale bars, 50 μ m. Arrows point to cell VE-4, an excitatory motor neuron to the ventral muscles, which is inhibited by VI-1 in standard saline. The arrows in succeeding panels indicate data from this motor neuron.

(B) Raster plots showing the optical signals from all circled cells in (A), with changes in fluorescence amplitude indicated by colors (calibration bar to the right of the raster plots).

(C) Polar plots showing the coherence phase (the angle from 0°) and magnitude (distance from the center) of the responses of all observed neurons. Values greater than the dashed line are coherent, at 95% confidence, with the stimulus.

(D) Number of neurons that showed significantly coherent responses to stimulation of a P_v cell relative to the total number of cells imaged in each experiment (mean \pm SEM for control): premanipulation control ($n = 13$), after adding BMI ($n = 7$), while hyperpolarizing the inhibitors ($n = 6$), and after each manipulation ($n = 13$). (* $p < 0.05$, *** $p < 0.001$ [one-way ANOVA, $F_{3,33} = 12.11$, a posteriori Tukey test]).

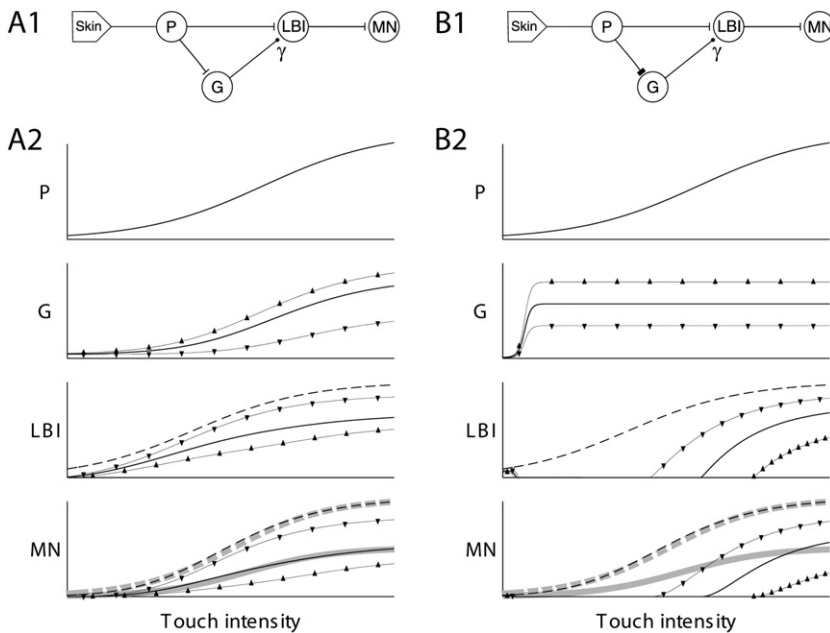


Figure 8. Modeling the Influence of Central GABAergic Inhibition on the Local Bend Response

(A) Model with feed-forward inhibition. (A1) Schematic of the modeled circuit. The model consists of one somatosensory P cell (P), one interneuron (LBI), one motor neuron (MN), and one GABAergic inhibitor (G). The T bars indicate excitatory connections, and black circles represent inhibitory connections. (A2) Activity of the modeled cells as a function of skin touch: with inhibition intact (solid black), with inhibition blocked (dashed black), with decreased inhibition (down-pointing triangles), and with increased inhibition (up-pointing triangles). For the black curves, the model parameters (slopes, locations of half-maximum response, and synaptic strengths) were chosen to make the output resemble the experimental results (gray lines in bottom panel: control, solid; with BMI, dashed).

(B) Model with saturating inhibition. (B1) Schematic. The thick T bar represents a stronger synapse between P and G. All other connections were the same as in (A). (B2) Activity of the modeled cells: with a medium amount of saturating inhibition (solid), increased inhibition (up-pointing triangles), reduced inhibition (down-pointing triangles), and no inhibition (dashed; identical to results in [A2] by construction). In this version of the model, increasing the activity of the G cell shifted the MN output left to right (solid lines in LBI and MN), unlike the experimental data (gray lines as in [A2]).

a motor neuron (MN). The responses of the sensory neuron (curve P) provided the input to the circuit, and the motor neuron responses (curves MN) were the output of the system. In the leech, there are approximately two dozen interneurons and motor neurons involved in the local bend reflex, so MN and LBI represent classes of neurons rather than single cells. To represent the generalized inhibition, we used a GABAergic cell (G), which is excited by the P cell and inhibits the interneuron with a synaptic strength γ . The firing rate of each cell is a simple sigmoidal function of its inputs, defined by only two parameters, a slope and a threshold. We examined the effect of the generalized GABAergic inhibition by varying the strength of the inhibitory synapses (γ) onto the interneuron. In particular, setting $\gamma = 0$ corresponds to complete blocking of GABAergic inhibition, corresponding to the application of BMI.

We chose connection strengths that produced an input/output function in the motor neuron that matched the behavioral data for the on-target region of the body wall (Figure 2A); the responses of the P, G, LBI, and MN neurons in this condition are shown as black lines in the graphs in Figure 8A2. With $\gamma = 0$ (i.e., no inhibition), the responses of LBI and MN increased in amplitude but did not shift along the “touch intensity” axis (dashed black lines). The model data closely matched the experimental data in control conditions (solid gray line) and after BMI application (dashed gray line). The gain of the model output could be controlled by altering the activation threshold of the GABAergic cell (thin black lines with triangle markers).

For GABAergic inhibition to result in a change of gain of the output, it was critical that the GABAergic cell (G) was activated over the same range of touch intensities as the P cell, and in the same manner. If, instead, the P-to-G synapse was so strong that the G cell activity saturated at low touch intensities (Fig-

ure 8B), the resulting G cell activity was effectively constant over most of the P cell activity range, producing a left-right shift of the MN output along the “touch intensity” axis (i.e., it had a subtractive effect) rather than a scaling (i.e., a multiplicative effect).

DISCUSSION

We found that the circuit producing local bending behavior in the leech recruits two types of inhibition to produce a precise localized response: a lateral inhibition through inhibitory motor neurons that restricts the contraction to the side that was stimulated, and a generalized inhibition, independent of the inhibitory motor neurons, that restricts the amplitude of the response in proportion to the intensity of stimulation.

The generalized increase in the amplitude of local bending during BMI application (Figure 2) was unexpected. The local bend circuit had been thought to be a broadly dispersed, feed-forward excitatory network from P cells to local bend interneurons, to motor neurons, with lateral inhibition only at the motor neuronal level to sharpen up the edges of the contraction and produce relaxation on the opposite side (Kristan et al., 1995; Lockery and Kristan, 1990b). Instead, the finding of a strong, generalized inhibition implies that the excitatory connections by themselves would produce a segment-wide contraction of all the longitudinal muscles, even at low stimulus intensity (Figures 3 and 4). This is indeed what was observed in embryonic leeches, before GABAergic inhibition is detectable (Marin-Burgin et al., 2005). The presence of this generalized inhibition means that all the motor neurons—even those that produce the contraction that is the active component of the bending response—normally receive a significant level of inhibition that strongly reduces

the excitation triggered by the stimulus. When we monitored the responses of individual motor neurons with intracellular recordings (Figures 5 and 6), we found exactly this: all excitors became significantly more active in the presence of BMI.

Producing scalable neuronal activity appears to be a property of many nervous systems, some much more complicated than that of the leech. For instance, a recent study on the rodent somatosensory cortex suggests that cortical circuits regulate their relative levels of excitation and inhibition across varying magnitudes of input (Higley and Contreras, 2006). Combined excitation and inhibition appears to be required for sensory processing not only in the somatosensory cortex (Gabernet et al., 2005; Wilentz and Contreras, 2005) but in visual (Priebe and Ferster, 2005), auditory (Wehr and Zador, 2003), and olfactory systems (Murphy et al., 2005; Yokoi et al., 1995). The level of inhibitory activity has long been recognized as a determinant of triggering seizure activity (Magloczky and Freund, 2005; Ribak et al., 1979), suggesting that a delicate balance of ongoing excitation and inhibition is important for normal functioning of the vertebrate brain. Modeling studies have found, for instance, that for activity to be able to propagate through a structure like the cortex without explosive activation requires a very narrow balance between excitation and inhibition (Vogels and Abbott, 2005). Our results indicate that even only moderately complex neuronal networks (Garcia-Perez et al., 2004) employ a balance between excitation and inhibition to produce useful behaviors.

The issue of gain control has become recognized as one of the most universal neural computational principles (Salinas and Thier, 2000). Previous studies had concluded that inhibition produced a linear shift in the input-output function of a neuron (a subtractive process) rather than a change in its slope (a divisive process). It has proven difficult to find cellular mechanisms that can change the gain of a system in a controlled way. For instance, pure inhibition produces a subtraction (i.e., a shift in the input/output function to a less sensitive part of the response range) rather than division (i.e., a decrease in the slope of the input/output function [Chance et al., 2002; Doiron et al., 2001]). In general, addition and subtraction are linear processes, whereas multiplication and division are nonlinear ones. Because it produces a nonlinear change in excitatory synaptic inputs, shunting inhibition has been proposed as a mechanism for division (Carandini and Heeger, 1994), but the effect of having a threshold for spiking acts to offset this nonlinearity and make the input/output function for spiking activity very nearly linear (Holt and Koch, 1997). Another mechanism proposed for multiplication is modulation of voltage-sensitive channels in the dendrites of cortical neurons by serotonin and norepinephrine (Heckman et al., 2003) because the active dendrites produce a nonlinearity that approximates multiplication (Heckman et al., 2005). Another, more systems-level mechanism for producing multiplication is to balance the overall level of excitation and inhibition so that the membrane potential of the neuron remains constant but the neuron becomes less responsive to a given input as the balanced excitation and inhibition increases (Chance et al., 2002).

Feedforward inhibition has been found, in several systems, to adjust the timing at which spikes occur (Blitz and Regehr, 2005; Mittmann et al., 2005; Pouille and Scanziani, 2001; Priebe and

Ferster, 2005; Wehr and Zador, 2003). Our results show that feedforward inhibition can also be used to adjust the gain of the circuit that triggers it. We found that a generalized feedforward inhibition onto the circuit produces a multiplication of the local bend response over the whole range of stimulus amplitudes, from threshold to saturation (Figure 2). Our simple model of parallel excitation and inhibition (Figure 8A) shows that a feedforward inhibitory circuit, activated in a graded manner by the sensory cells, can change the gain of the local bending circuit and therefore could explain the results of physiological experiments with GABA blockers (Figure 2), whereas a saturating inhibitory circuit (Figure 8B) failed to reproduce the experimental results. It is possible that modulation of this feedforward inhibitory circuit, represented by G in the circuits of Figure 8, could be partially responsible for the suppression of the local bend response during other behaviors such as feeding (Misell et al., 1998).

EXPERIMENTAL PROCEDURES

Leech Care

Adult medicinal leeches (*Hirudo* sp.) from Carolina Biological Supply Co. (Burlington, NC) and Leeches USA (Westbury, NY) were maintained in a cool room (15°C; 12 hr light/dark cycle) in 5 gallon aquaria containing Instant Ocean Sea Salt (Aquarium Systems, Mentor, OH; diluted 1:1000 with deionized water). They weighed 2.0–5.0 g and had not eaten for at least 4 weeks.

Body Wall Preparations

To dissect the leeches, we used ice-cold leech saline (Muller et al., 1981) to anesthetize them. To perform experiments, we used saline at room temperature (20°C–22°C). Body wall preparations produced reliable local bends for longer than 4 hr. To reduce variability, we always used segment 10 of the 21 midbody segments. We waited at least 3 min between stimuli to avoid sensitizing or habituating motor responses (Lockery and Kristan, 1991). We used body wall preparations similar to those used previously (Baca et al., 2005; Kristan, 1982; Nicholls and Baylor, 1968), consisting of three segments removed from the leech midbody region (Figure 1A) and cut along the dorsal midline. We removed the anterior and posterior ganglia, leaving only the central segment innervated by a single ganglion, then flattened the body wall and pinned it skin-side up on a plastic Petri dish coated with Sylgard (Dow Corning, Midland, MI; Figures 1B and 1C). We used these preparations to record behavioral movements (Figure 2). To apply drugs to either the ganglion or the body wall selectively, we used a *split body wall preparation*, in which we additionally cut along the ventral body wall, leaving the ganglion attached to the left and right halves (Figure 3A); we then formed a water-tight Vaseline well around the ganglion through which the lateral nerve roots passed. To record from neurons and stimulate them individually, we used a *hole-in-the-wall preparation*, in which the opening in the ventral body wall was limited to a small hole just over the ganglion (Figure 4C). For the experiments using voltage-sensitive dyes, we used a single isolated ganglion dissected free of the body wall entirely and pinned to the Sylgard in a Petri dish. In some electrophysiological and all imaging experiments, we removed the connective tissue capsule and the glial packets that encase the neuronal somata to ease cell impalements and to deliver both drugs and voltage-sensitive dyes.

We recorded intracellularly from neuronal somata with sharp glass microelectrodes (20–30 M Ω filled with 3 M potassium acetate). We identified motor neurons by their location, size, and electrophysiological properties (Stuart, 1970) and delivered current-clamp pulses using an Axoclamp 2-A amplifier controlled with Axograph 4.9 (Axon Instruments, now Molecular Devices, Sunnyvale, CA) on a PowerPC G3 computer (Apple, Cupertino, CA). We removed all the inhibitory effects produced by the inhibitory motor neurons by passing strong hyperpolarization (–2 to –7 nA) into one inhibitory motor neuron (Granzow et al., 1985; Lockery and Kristan, 1990b); this works because all the inhibitory motor neurons are electrically coupled to one another (Figure 4B).

Delivery of GABA Blockers

Preliminary experiments using bicuculline methiodide (BMI), SR 95531 (“GABazine”), and picrotoxin showed that only BMI blocked the inhibition from inhibitory motor neurons onto excitatory motor neurons, a synapse known to be GABAergic (Cline, 1986); we therefore used only BMI to block inhibitory transmission. BMI is known to block calcium-activated potassium channels responsible for afterhyperpolarization in a variety of mammalian preparations, thereby increasing the excitability of the neurons (Seutin and Johnson, 1999). We saw no evidence for such effects on leech neurons; in fact, a previous study (Cline, 1986) as well as our own control experiments (in the section on GABAergic Inhibition) found that BMI slightly hyperpolarized leech motor neurons, thereby *decreasing* their excitability. We delivered BMI (Sigma-Aldrich) to the ganglion by a gravity-fed drip system at a concentration of 0.1 mM. Initial experiments showed that this concentration produced complete block of the central inhibition among the motor neurons, but did not block the inhibitory neuromuscular junctions in the body wall.

Stimulus: Force Controller

As described previously (Baca et al., 2005), we used a Dual-Mode Lever Arm System (“poker”; Aurora Scientific, Ontario, Canada, Model 300B) to deliver tactile stimuli at a chosen force (0.75–400 mN) to the leech body wall using a 1 mm diameter bead of epoxy on the tip of a 27 ga needle (Figure 1A). We mounted the head stage of the force controller on a micromanipulator (Narishige International, East Meadow, NY). The stimuli produced a range of local bend responses similar to the bends produced in earlier studies using smaller forces with smaller-tipped filaments (Garcia-Perez et al., 2004; Lewis and Kristan, 1998a, 1998b; Zoccolan and Torre, 2002).

Terminology

We have chosen to use the terms “ipsilateral” and “contralateral” to indicate the locations of the peripheral fields of sensory and motor neurons rather than to indicate the locations of their somata within the ganglion. This preserves their functional connectivity: each mechanosensory P (pressure-sensitive) cell excites its ipsilateral excitatory motor neuron, even though the somata are on opposite sides of the ganglion. In addition, we use the term “on-target” to refer to the motor neurons that contract the body wall in the *same* area of body wall innervated by the stimulated P cell, and “off-target” to refer to the motor neurons that contract muscles on the body wall directly opposite (Figures 4A and 5). The areas between these two are called “intermediate” in location. Each longitudinal muscle motor neuron is identified by three features: (1) the location of the longitudinal muscle it innervates (D, dorsal; V, ventral), (2) whether it excites the muscle or inhibits it (E or I), and (3) the number assigned to its soma on the standard ganglionic map (Muller et al., 1981). Hence, cell DI-1 inhibits dorsal longitudinal muscles, and its soma is in map location 1. For brevity, we sometimes use the terms “excitator” and “inhibitor” in place of “excitatory longitudinal muscle motor neuron” and “inhibitory longitudinal muscle motor neuron.”

Behavioral Video Recordings

We recorded the image of the body wall preparation (Figures 1B and 1C) through a Wild dissection microscope using a C-Mounted Hitachi KP-M1 monochrome CCD camera (Image Labs International, Bozeman, MT). We captured the images (640 × 480 pixel resolution) at 10 Hz and digitized using a Data Translation frame grabber card (DT3155) controlled with the MATLAB (The Mathworks, Natick, MA) Image Acquisition Toolbox on a PC computer (Figure 1A). On a different computer, pulses from Axograph 4.9 software (Axon Instruments, Union City, CA) synchronized video acquisition with the stimulus controller and the electrical recordings. As previously described (Baca et al., 2005), we tracked the body wall motion by making optic flow estimates between successive image frames (Lucas and Kanade, 1981; Ye and Haralick, 2000). We captured 20 to 40 images that include the onset of the bend, then calculated optic flow fields between successive frames.

To minimize the effects of restraining the preparation in behavioral studies, we pinned the body wall only in the denervated anterior and posterior ends (Figure 1B). In these preparations, we measured local bending responses along anterior-posterior lines in the five innervated annuli at four locations: on-target ventral (V_{on}) and three off-target sites (ventral [V_{off}], lateral [L_{off}],

and dorsal [D_{off}]). (The lateral and dorsal movements ipsilateral to the stimulus were distorted by the movements of the stimulator arm and could not be measured reliably.) We manually marked points along the edges of the five annuli corresponding to the innervated segment in the first frame of each of the resulting movies, then used the optic flow detection algorithm (Ye and Haralick, 2000) to track the motion of these markers. We delivered mechanical stimuli of 3 s duration spaced 3 min apart to prevent response adaptation. The actual force applied was verified using a lab balance placed under the Petri dish. In this manner, forces as low as 1 mN could be applied with less than 10% variability.

To record electrophysiologically, we needed to pin the preparation tightly along all four of its margins (Figure 1C). The contractions at the site of stimulation were readily visible; they were smaller than those recorded in less constrained preparations but were qualitatively similar. The relaxations contralateral to the site of stimulation, however, were often not visible. To measure local bending in these preparations, we selected a rectangular region of interest (ROI) that showed robust movement and was free from edge or pinning artifacts (Figure 1C). The ROI spanned one to two annuli along the long axis of the leech and included its entire circular axis. For a given preparation, we used the same ROI for all trials. Because we were most interested in the contribution to local bending produced by the longitudinal muscles, we calculated only that component of the movement that ran parallel to the leech’s long axis.

Quantification of Behavior

In the loosely pinned preparations (Figure 1B), we compared the distance between anterior and posterior markers 0.5 s after withdrawal of the stimulator to the distance just before stimulation. The recording below the trace is one smoothed response to a stimulus at V_{on} in the middle of the intensity range used, with the length measurement normalized to the average length of an annulus (annuli are elevations in the skin of the body wall that run circumferentially around the body; five annuli constitute one segment). In the tightly stretched preparations (Figure 1C), the stimulus lasted 0.5 s, and the response peaked at about 1.0 s after stimulus offset; we therefore used the cumulative motion profile at the peak of the response, in units of annulus widths. We smoothed these motion profiles with a Gaussian filter. We measured the magnitude of the responses as their peak amplitudes because, although it is only a single measure of each response, it is the closest behavioral counterpart to the peak firing rate of the motor neurons responsible for longitudinal muscle contractions (Mason and Kristan, 1982).

Monitoring the Electrical Activity of Multiple Neurons Using Voltage-Sensitive FRET Dyes

We stained dissected, isolated ganglia from adult leeches with a pair of FRET dyes: 10 μ M imyristin of the donor, coumarin [*N*-(6-chloro-7-hydroxycoumarin-3-carbonyl)-imyristoylphosphatidylethanolamine] and 12.5 μ M of the acceptor, oxonol [bis (1,3-diethyl-thiobarbiturate)-trimethine oxonol], both from Vertex Pharmaceuticals Inc., San Diego, CA. For details of their preparation and application, see Cacciatore et al. (1999) and Taylor et al. (2003). We acquired fluorescence images using an upright microscope (Axioskop 2FS; Zeiss, Thornwood, NY) equipped with a 40 \times , 0.8 NA water-immersion objective (Achromplan; Zeiss). For epi-illumination we used a tungsten halogen lamp (64625 HLX; Osram Sylvania, Danvers, MA) in standard housing (HAL 100; Zeiss), powered by a low-ripple power supply (JQE 15-12M; Kepco, Flushing, NY). For all voltage-sensitive dye imaging, we acquired images only at the coumarin emission wavelength. The filter set consisted of a 405 \pm 15 nm band-pass excitation filter, a 430 nm dichroic mirror, and a 460 \pm 25 nm band-pass emission filter (Chroma Technology Corporation, Brattleboro, VT). We acquired the optical data using a water-cooled CCD camera (MicroMax 512 BFT; Roper Scientific, Tucson, AZ) operated in frame-transfer mode at a frame rate of 20 Hz. The CCD chip in this camera has 512 \times 512 pixels, but we binned at 4 \times 4 pixels to yield a 128 \times 128 pixel image. The CCD chip was maintained at -25° C during imaging. Images were stored using the software package Win-View/32 (Roper Scientific, Trenton, NJ). The combination of coumarin and oxonol yielded sensitivities of 5%–20% change in fluorescence/100 mV for 1 Hz square-wave voltage signals with a 10 mV amplitude, centered around a resting potential of -50 mV.

Image Analysis

We analyzed the images using a custom-made graphic user interface in Matlab. We averaged all pixels within each cellular outline in each frame (Taylor et al., 2003). To find neurons responding to a stimulated mechanosensory neuron, we impaled the sensory neuron's soma with a microelectrode and passed a train of current pulses (4 nA, 7 ms, 15 Hz) for 500 ms each second while simultaneously collecting images at 20 Hz for 10 s. We always impaled a postsynaptic cell to compare optical data with intracellular recordings. Using coherence analysis (coherence is essentially a correlation of two trajectories at the dominant shared frequency, in this case 1 Hz), we identified neurons whose optical signals were correlated with the stimulated one (Cacciatore et al., 1999). In some experiments, a 100 μ M BMI solution was applied to the ganglion; images were taken before and during BMI application. We then washed out the BMI solution for 10 min and obtained a post-wash recording.

Statistics

We applied standard statistical tests to our data (one-way ANOVA, a posteriori Tukey test; MANOVA for multivariate data, and corrected one-tailed and two-tailed t tests where appropriate) using the Statistics Toolbox in MatLab. All values listed are mean \pm SEM.

Modeling Input-Output Functions of the Neurons in the Local Bend Circuitry

The P cell in the model was activated by skin touch using a sigmoidal of the form

$$P(F) = 1/2 + 1/2 \tanh(\alpha_P \log(F/\theta_P)),$$

where F is the touch force (in milliNewtons), $\theta_P = 25$ mN, and $\alpha_P = 0.3$.

The activation of the other cells was modeled using sigmoidal functions of their synaptic inputs:

$$G(P) = 1/(1 + (\theta_G/P)^{\alpha_G}),$$

$$I(P, G) = 1/(1 + (\theta_I/(P + \gamma G))^{\alpha_I}) + I_0,$$

and

$$M(I) = 1/(1 + (\theta_M/I)^{\alpha_M}).$$

To match the experimental results (black curves in Figure 8A), we used $\theta_G = 1.4$, $\alpha_G = 1.7$, $\theta_I = 0.4$, $\alpha_I = 1.1$, $I_0 = 0.02$, $\theta_M = 1.4$, $\alpha_M = 1.9$, and $\gamma = 1.65$.

ACKNOWLEDGMENTS

We thank our colleague, Massimo Scanziani, for helpful suggestions in preparing the manuscript. The research was supported by an NIH research grants MH43396 and NS35336 (W.B.K.) and by gifts from the Microsoft Research Laboratory and Richard Geckler and by an NRSA award (MH13037) to S.M.B.

Received: March 20, 2006

Revised: August 22, 2007

Accepted: November 28, 2007

Published: January 23, 2008

REFERENCES

- Abbott, L.F., and Chance, F.S. (2005). Drivers and modulators from push-pull and balanced synaptic input. *Prog. Brain Res.* 149, 147–155.
- Baca, S.M., Thomson, E.E., and Kristan, W.B. (2005). Location and intensity discrimination in the leech local bending response quantified using optic flow and principal components analysis. *J. Neurophysiol.* 93, 3560–3572.
- Berg, R.W., Alaburda, A., and Hounsgaard, J. (2007). Balanced inhibition and excitation drive spike activity in spinal half-centers. *Science* 315, 390–393.
- Blitz, D.M., and Regehr, W.G. (2005). Timing and specificity of feed-forward inhibition within the LGN. *Neuron* 45, 917–928.
- Briggman, K.L., Abarbanel, H.D.I., and Kristan, W.B., Jr. (2005). Optical imaging of neuronal populations during decision-making. *Science* 307, 896–901.
- Buneo, C.A., and Andersen, R.A. (2006). The posterior parietal cortex: Sensorimotor interface for the planning and online control of visually guided movements. *Neuropsychologia* 44, 2594–2606.
- Cacciatore, T.W., Brodfuehrer, P.D., Gonzalez, J.E., Jiang, T., Adams, S.R., Tsien, R.Y., Kristan, W.B., and Kleinfeld, D. (1999). Identification of neural circuits by imaging coherent electrical activity with FRET-based dyes. *Neuron* 23, 449–459.
- Carandini, M., and Heeger, D.J. (1994). Summation and division by neurons in primate visual cortex. *Science* 264, 1333–1336.
- Chance, F.S., Abbott, L.F., and Reyes, A.D. (2002). Gain modulation from background synaptic input. *Neuron* 35, 773–782.
- Cline, H. (1986). Evidence for GABA as a neurotransmitter in the leech. *J. Neurosci.* 6, 2848–2856.
- Cline, H.T., Nusbaum, M.P., and Kristan, W.B., Jr. (1985). Identified GABAergic inhibitory motor neurons in the leech central nervous system take up GABA. *Brain Res.* 348, 359–362.
- Connor, C.E., Preddie, D.C., Gallant, J.L., and Van Essen, D.C. (1997). Spatial attention effects in macaque area V4. *J. Neurosci.* 17, 3201–3214.
- Doiron, B., Longtin, A., Berman, N., and Maler, L. (2001). Subtractive and divisive inhibition: effect of voltage-dependent inhibitory conductances and noise. *Neural Comput.* 13, 227–248.
- Dunn, F.A., and Rieke, F. (2006). The impact of photoreceptor noise on retinal gain controls. *Curr. Opin. Neurobiol.* 16, 363–370.
- Eccles, J.C. (1969). *The Inhibitory Pathways of the Central Nervous System* (Springfield, IL: Thomas).
- Gabernet, L., Jadhav, S.P., Feldman, D.E., Carandini, M., and Scanziani, M. (2005). Somatosensory integration controlled by dynamic thalamocortical feed-forward inhibition. *Neuron* 48, 315–327.
- Garcia-Perez, E., Zoccolan, D., Pinato, G., and Torre, V. (2004). Dynamics and reproducibility of a moderately complex sensory-motor response in the medicinal leech. *J. Neurophysiol.* 92, 1783–1795.
- Granzow, B., and Kristan, W.B., Jr. (1986). Inhibitory connections between motor neurons modify a centrally generated motor pattern in the leech *hirudo-medicinalis* nervous system. *Brain Res.* 369, 321–325.
- Granzow, B., Friesen, W., and Kristan, W., Jr. (1985). Physiological and morphological analysis of synaptic transmission between leech motor neurons. *J. Neurosci.* 5, 2035–2050.
- Haider, B., Duque, A., Hasenstaub, A.R., and McCormick, D.A. (2006). Neocortical network activity in vivo is generated through a dynamic balance of excitation and inhibition. *J. Neurosci.* 26, 4535–4545.
- Hatton, G.I. (1998). Synaptic modulation of neuronal coupling. *Cell Biol. Int.* 22, 765–780.
- Heckman, C.J., Lee, R.H., and Brownstone, R.M. (2003). Hyperexcitable dendrites in motoneurons and their neuromodulatory control during motor behavior. *Trends Neurosci.* 26, 688–695.
- Heckman, C.J., Gorassini, M.A., and Bennett, D.J. (2005). Persistent inward currents in motoneuron dendrites: Implications for motor output. *Muscle Nerve* 31, 135–156.
- Heinzel, H., Weimann, J., and Marder, E. (1993). The behavioral repertoire of the gastric mill in the crab, *Cancer pagurus*: an in situ endoscopic and electrophysiological examination. *J. Neurosci.* 13, 1793–1803.
- Higley, M.J., and Contreras, D. (2006). Balanced excitation and inhibition determine spike timing during frequency adaptation. *J. Neurosci.* 26, 448–457.
- Holt, G.R., and Koch, C. (1997). Shunting inhibition does not have a divisive effect on firing rates. *Neural Comput.* 9, 1001–1013.
- Kristan, W.B., Jr. (1982). Sensory and motor neurons responsible for the local bending response in leeches. *J. Exp. Biol.* 96, 161–180.
- Kristan, W.B., Jr., McGirr, S.J., and Simpson, G.V. (1982). Behavioral and mechanosensory neuron responses to skin stimulation in leeches. *J. Exp. Biol.* 96, 143–160.

- Kristan, W.B., Jr., Lockery, S.R., and Lewis, J.E. (1995). Using reflexive behaviors of the medicinal leech to study information processing. *J. Neurobiol.* **27**, 380–389.
- Kuffler, S.W. (1953). Discharge patterns and functional organization of mammalian retina. *J. Neurophysiol.* **16**, 37–68.
- Lewis, J.E., and Kristan, W.B., Jr. (1998a). A neuronal network for computing population vectors in the leech. *Nature* **391**, 76–79.
- Lewis, J.E., and Kristan, W.B., Jr. (1998b). Quantitative analysis of a directed behavior in the medicinal leech: implications for organizing motor output. *J. Neurosci.* **18**, 1571–1582.
- Lockery, S., and Kristan, W., Jr. (1990a). Distributed processing of sensory information in the leech. I. Input-output relations of the local bending reflex. *J. Neurosci.* **10**, 1811–1815.
- Lockery, S.R., and Kristan, W.B., Jr. (1990b). Distributed processing of sensory information in the leech II. Identification of interneurons contributing to the local bending reflex. *J. Neurosci.* **10**, 1816–1829.
- Lockery, S.R., and Kristan, W.B., Jr. (1991). Two forms of sensitization of the local bending reflex of the medicinal leech. *J. Comp. Physiol. [A]* **168**, 165–177.
- Lucas, B.D., and Kanade, T. (1981). An iterative image registration technique with an application to stereo vision (DARPA). Paper presented at: Proceedings of the 1981 Image Understanding Workshop.
- Maglóczky, Z., and Freund, T.F. (2005). Impaired and repaired inhibitory circuits in the epileptic human hippocampus. *Trends Neurosci.* **28**, 334–340.
- Mamiya, A., Manor, Y., and Nadim, F. (2003). Short-term dynamics of a mixed chemical and electrical synapse in a rhythmic network. *J. Neurosci.* **23**, 9557–9564.
- Marin-Burgin, A., Eisenhart, F.J., Baca, M.S., Kristan, W.B., Jr., and French, K.A. (2005). Sequential development of electrical and chemical synaptic connections generates a specific behavioral circuit in the leech. *J. Neurosci.* **25**, 2478–2489.
- Mason, A., and Kristan, W.B., Jr. (1982). Neuronal excitation, inhibition, and modulation of leech longitudinal muscle. *J. Comp. Physiol. [A]* **146**, 527–536.
- McAdams, C.J., and Maunsell, J.H.R. (1999). Effects of attention on the reliability of individual neurons in monkey visual cortex. *Neuron* **23**, 765–773.
- Misell, L.M., Shaw, B.K., and Kristan, W.B., Jr. (1998). Behavioral hierarchy in the medicinal leech, *Hirudo medicinalis*: Feeding as a dominant behavior. *Behav. Brain Res.* **90**, 13–21.
- Mittmann, W., Koch, U., and Häusser, M. (2005). Feed-forward inhibition shapes the spike output of cerebellar Purkinje cells. *J. Physiol.* **563**, 369–378.
- Moss, B.L., Fuller, A.D., Sahley, C.L., and Burrell, B.D. (2005). Serotonin modulates axo-axonal coupling between neurons critical for learning in the leech. *J. Neurophysiol.* **94**, 2575–2589.
- Muller, K.J., Nicholls, J.G., and Stent, G.S. (1981). *Neurobiology of the Leech* (Cold Spring Harbor, NY: Cold Spring Harbor Laboratory).
- Murphy, G.J., Darcy, D.P., and Isaacson, J.S. (2005). Intraglomerular inhibition: signaling mechanisms of an olfactory microcircuit. *Nat. Neurosci.* **8**, 354–364.
- Nicholls, J.G., and Baylor, D.A. (1968). Specific modalities and receptive fields of sensory neurons in CNS of the leech. *J. Neurophysiol.* **31**, 740–756.
- Nicholls, J.G., and Purves, D. (1970). Monosynaptic chemical and electrical connections between sensory and motor cells in the central nervous system of the leech. *J. Physiol.* **209**, 647–667.
- Ort, C.A., Kristan, W.B., Jr., and Stent, G.S. (1974). Neuronal control of swimming in the medicinal leech part 2 identification and connections of motor neurons. *J. Comp. Physiol.* **94**, 121–154.
- Pouille, F., and Scanziani, M. (2001). Enforcement of temporal fidelity in pyramidal cells by somatic feed-forward inhibition. *Science* **293**, 1159–1163.
- Priebe, N.J., and Ferster, D. (2005). Direction selectivity of excitation and inhibition in simple cells of the cat primary visual cortex. *Neuron* **45**, 133–145.
- Ribak, C.E., Harris, A.B., Vaughn, J.E., and Roberts, E. (1979). Inhibitory, GABAergic nerve terminals decrease at sites of focal epilepsy. *Science* **205**, 211–214.
- Salinas, E., and Abbott, L.F. (1997). Invariant visual responses from attentional gain fields. *J. Neurophysiol.* **77**, 3267–3272.
- Salinas, E., and Thier, P. (2000). Gain modulation: a major computational principle of the central nervous system. *Neuron* **27**, 15–21.
- Seutin, V., and Johnson, S.W. (1999). Recent advances in the pharmacology of quaternary salts of bicuculline. *Trends Pharmacol. Sci.* **20**, 268–270.
- Shadlen, M.N., and Newsome, W.T. (1994). Noise, neural codes and cortical organization. *Curr. Opin. Neurobiol.* **4**, 569–579.
- Stent, G.S., Kristan, W.B., Jr., Friesen, W.O., Ort, C.A., Poon, M., and Calabrese, R.L. (1978). Neuronal generation of the leech swimming movement an oscillatory network of neurons driving a loco motory rhythm has been identified. *Science* **200**, 1348–1357.
- Stevens, C.F., and Zador, A.M. (1998). Input synchrony and the irregular firing of cortical neurons. *Nat. Neurosci.* **1**, 210–217.
- Stuart, A.E. (1969). Excitatory and inhibitory motoneurons in the central nervous system of the leech. *Science* **165**, 817–819.
- Stuart, A.E. (1970). Physiological and morphological properties of motoneurons in the central nervous system of the leech. *J. Physiol.* **209**, 627–646.
- Taylor, A.L., Cottrell, G.W., Kleinfeld, D., and Kristan, W.B., Jr. (2003). Imaging reveals synaptic targets of a swim-terminating neuron in the leech CNS. *J. Neurosci.* **23**, 11402–11410.
- Thomson, E.E., and Kristan, W.B. (2006). Encoding and decoding touch location in the leech CNS. *J. Neurosci.* **26**, 8009–8016.
- Vogels, T.P., and Abbott, L.F. (2005). Signal propagation and logic gating in networks of integrate-and-fire neurons. *J. Neurosci.* **25**, 10786–10795.
- Wehr, M., and Zador, A.M. (2003). Balanced inhibition underlies tuning and sharpens spike timing in auditory cortex. *Nature* **426**, 442–446.
- Wilent, W.B., and Contreras, D. (2005). Dynamics of excitation and inhibition underlying stimulus selectivity in rat somatosensory cortex. *Nat. Neurosci.* **8**, 1364–1370.
- Wolfart, J., Debay, D., Le Masson, G., Destexhe, A., and Bal, T. (2005). Synaptic background activity controls spike transfer from thalamus to cortex. *Nat. Neurosci.* **8**, 1760–1767.
- Ye, M., and Haralick, R.M. (2000). Image flow estimation using facet model and covariance propagation. In *Vision Interface: Real World Applications of Computer Vision*, Y.H. Yang and M. Cheriet, eds. (Hackensack, NJ: World Scientific Pub Co), pp. 209–241.
- Yokoi, M., Mori, K., and Nakanishi, S. (1995). Refinement of odor molecule tuning by dendrodendritic synaptic inhibition in the olfactory bulb. *Proc. Natl. Acad. Sci. USA* **92**, 3371–3375.
- Zoccolan, D., and Torre, V. (2002). Using optical flow to characterize sensory-motor interactions in a segment of the medicinal leech. *J. Neurosci.* **22**, 2283–2298.